Biol. Cybern. 71, 153–160 (1994)

Biological Cybernetics

© Springer-Verlag 1994

In-phase and antiphase self-oscillations in a model of two electrically coupled pacemakers

G. S. Cymbalyuk, E. V. Nikolaev, R. M. Borisyuk

Institute of Mathematical Problems of Biology, Russian Academy of Sciences, Pushchino, Moscow Region 142292, Russian Federation

Received: 8 December 1992/Accepted in revised form: 22 January 1994

Abstract. The dynamic behavior of a model of two electrically coupled oscillatory neurons was studied while the external polarizing current was varied. It was found that the system with weak coupling can demonstrate one of five stable oscillatory modes: (1) in-phase oscillations with zero phase shift; (2) antiphase oscillations with half-period phase shift; (3) oscillations with any fixed phase shift depending on the value of the external polarizing current; (4) both in-phase and antiphase oscillations for the same current value, where the oscillation type depends on the initial conditions; (5) both in-phase and quasiperiodic oscillations for the same current value. All of these modes were robust, and they persisted despite small variations of the oscillator parameters. We assume that similar regimes, for example antiphase oscillations, can be detected in neurophysiological experiments. Possible applications to central pattern generator models are discussed.

1 Introduction

In this paper we consider the dynamic behavior of a model of two identical, electrically coupled pacemakers. The dependence of the oscillatory regimes of the system upon the input polarizing current was investigated. A slightly modified Hindmarsh-Rose model is used to describe each oscillatory neuron in terms of its membrane potential and a recovery variable (Hindmarsh and Rose 1984). The weak electrical coupling between the oscillators is represented by a term proportional to the difference between the membrane potentials of the two neurons.

Recent experimental evidence provides a basis for a number of hypotheses placing emphasis on the significance of gap junctions between neurons for visual information processing, learning and ontogenesis (for review see Constantine-Paton et al. 1990; Yang et al. 1990; Yuste et al. 1992; Dermietzel and Spray 1993). This aspect should also be relevant to movement control, in particular in relation to central pattern generation (CPG). The existence of both electrical coupling and endogenous oscillators in rhythm generation was clearly shown for many invertebrate and vertebrate CPGs (Arshavsky et al. 1985; Selverston and Moulins 1985; Getting 1988; Grillner and Matsushima 1991; Marder et al. 1992).

The systems of coupled oscillators underlying rhythm generation have been studied by many authors from both the experimental and the theoretical points of view (Kopell 1988; Rand et al. 1988; Schöner et al. 1990; Müller and Cruse 1991; Taga et al. 1991; Collins and Stewart 1993). Many papers on neural oscillators are devoted to the study of modes phase-locking in the case of weak coupling between oscillators (e.g., Aronson et al. 1990; Ermentrout and Kopell 1991; Borisyuk et al. 1992). In particular, it was shown by computer simulation (Kawato et al. 1979) that for two Van der Pol oscillators with electrical coupling, both in-phase and antiphase oscillations exist for the same parameter values, and the oscillation regime depends on the initial conditions. In previous papers (Borisyuk et al. 1992; Khibnik et al. 1992), the oscillatory regimes of two interacting identical Wilson-Cowan oscillators have been analyzed; it was shown, for example, that antiphase oscillations are stable for weak connections between excitatory neural populations.

Here, we consider the model of two coupled oscillators described by a system of four ordinary differential equations. The approach developed here allows us to enumerate the oscillatory regimes of the system and to describe transitions from one regime to another due to parameter variation.

It was found that this system of two identical oscillators with fixed weak electrical coupling can show one of five stable oscillatory modes: (1) in-phase oscillations with zero phase shift; (2) antiphase oscillations with half-period phase shift; (3) oscillations with any intermediate phase shift, the value of which depends on the value of the external polarizing current; (4) both in-phase and antihase oscillations for the same parameter value, where

Correspondence to: G. S. Cymbalyuk

the oscillation type depends on the initial conditions; (5) both in-phase and quasiperiodic oscillations for the same parameter value.

It is important to note that for a fixed coupling type and a small value of connection strength, we use the input polarizing current as a control parameter. Each value of this parameter is associated with one of the five different types of oscillatory behavior.

The model was studied by the methods of bifurcation theory. Bifurcation diagrams of periodical solutions have been used to analyze oscillation stability. To compute the diagrams, we employ both the numerical technique of path continuation (Khibnik et al. 1993) and an asymptotic method when the value of the connection strength tends to zero. The bifurcation diagrams allow us to trace transitions from one regime to another with variation of the input current. This provides the background for designing mechanisms of controlling the system.

The numerical analysis of limit cycle bifurcations was performed by the LOCBIF program (Khibnik et al. 1993). The software implementation of the asymptotic method was used to find periodic solutions and to determine their stability for weak coupling strengths.

In Sect. 2, we describe in detail a system of two identical endogenous oscillators introduced by Hindmarsh and Rose (1984).

In Sect. 3, we describe the bifurcation diagrams of limit cycles for a small fixed value of connection strength and the bifurcations of limit cycles in the case when the connection strength tends to zero (asymptotic method) and compare the results obtained by the numerical and asymptotic methods.

In Sect. 4, we discuss possible applications of the results. The presence of robust, antiphase oscillations in the model of coupled pacemaker neurons implies that analogous oscillations may occur in neurophysiological experiments as well.

In the Appendix, we provide the mathematical basis and the numerical algorithm for the asymptotical method applied.

2 A model

A single oscillator is a model of a neuron capable of rhythmic activity generation (Hindmarsh and Rose 1984). Let $E(t)$ be the membrane potential and let $I(t)$ be a recovery variable. Then the dynamics of neuron's activity is given by

$$\begin{aligned} \frac{dE}{dt} &= \frac{1}{C}(I - P(E)) \\ \frac{dI}{dt} &= Q(E) - I \end{aligned} \tag{1}$$

where C is the membrane capacity (below we set $C = 2$); $P(x) = x^3 - 3x^2 - I_0$; $Q(x) = -5x^2 + 1$; I_0 is the parameter determining the value of the input external current on the neuron membrane. The polynomials $P(x)$ and $Q(x)$ are derived by Hindmarsh and Rose (1982, 1984) by using voltage clamp data obtained from an oscillating neuron of the visceral ganglion of a pond snail.

We studied the model for the values of a dimensionless parameter I_0 in the range where system (1) has a stable limit cycle. Figure 1 shows the bifurcation diagrams of equilibria and limit cycle of a single oscillator under the variation of the parameter I_0. At $I_0 = -0.57$ and $I_0 = 7.9$, the equilibrium loses its stability (Andronov-Hopf bifurcation) and produces a limit cycle, which exists for $I_0 \in (-0.57, 7.9)$ and disappears via backward Andronov-Hopf bifurcation at $I_0 = 7.9$.

So, let us enumerate the stable regimes of a single oscillator for I_0 continuously varying from -1 to $+8$:

$(-1, -0.57)$ a bistable regime of two equilibria with high and low levels of membrane potential
$(-0.57, 0.19)$ both an oscillatory regime and an equilibrium with a low level of membrane potential
(0.19, 7.9) an oscillatory regime
(7.90, 8.0) an equilibrium

Consider now two identical, electrically coupled neuron oscillators. The dynamics of their activity is given by

$$\begin{aligned} \frac{dE_1}{dt} &= \frac{1}{C}(I_1 - P(E_1)) + \alpha(E_2 - E_1) \\ \frac{dI_1}{dt} &= Q(E_1) - I_1 \\ \frac{dE_2}{dt} &= \frac{1}{C}(I_2 - P(E_2)) + \alpha(E_1 - E_2) \\ \frac{dI_2}{dt} &= Q(E_2) - I_2 \end{aligned} \tag{2}$$

where $E_i(t)$ is the membrane potential of the ith oscillator ($i = 1, 2$), $I_i(t)$ is a recovery variable of the ith oscillator ($i = 1, 2$), P and Q are defined above, and α is the coupling strength between the oscillators ($0 < \alpha \ll 1$).

The assumption that the electrical coupling α is small is based on two experimentally observable situations: two neurons are close or their contact surface is sufficiently large; and two cells are coupled through a special electrical contact with large resistance.

Weak electrical coupling between oscillatory neurons has been found, for example, in the CPG of a swimming lamprey (Grillner and Matsushima 1991).

3 Results

To investigate the dynamic behavior of system (2), we analyzed the bifurcation diagrams of limit cycles while varying the parameter I_0. To compute the diagrams we used two methods: (a) a numerical technique of path continuation for the small fixed value of connection strength $\alpha = 0.05$; (b) an asymptotic method of expansion in series of a periodical solution when the small parameter α tends to zero. The former is more general and allows us to find different limit cycles and define their

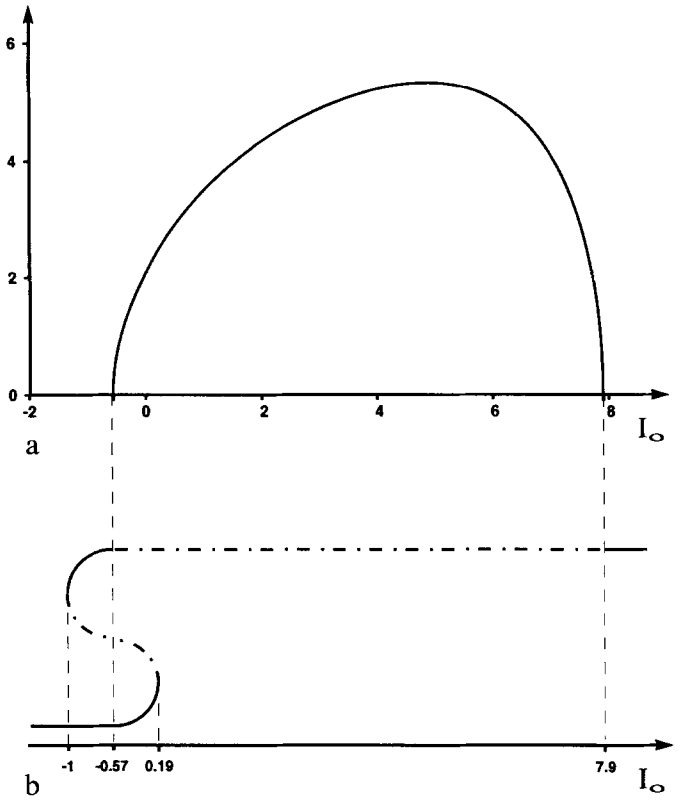

Fig. 1. Amplitude of a limit cycle (**a**) and stationary states (**b**) of a single oscillator versus the parameter I_0. A *solid line* corresponds to a stable regime, a *dash-dot line* to an unstable one

stability. The latter can be used only for the analysis of limit cycles lying on the two-dimensional invariant torus.

3.1 Invariant sets of the model

Before describing the bifurcation diagram, let us consider the invariant sets of system (2). If $\alpha = 0$, we can consider a product of the two independent, identical oscillators. If parameter I_0 belongs to the interval (0.19, 7.9), then the single oscillator has a stable limit cycle **C** and an unstable equilibrium **O**. Therefore, the following invariant sets exist, being products of these regimes:

- an equilibrium $\mathbf{O}_s = \mathbf{O} \times \mathbf{O}$
- a pair of nonsymmetric limit cycles, $\mathbf{NSC}_1 = \mathbf{O} \times \mathbf{C}$ and $\mathbf{NSC}_2 = \mathbf{C} \times \mathbf{O}$
- an invariant 2-torus $\mathbb{T}^2 = \mathbf{C} \times \mathbf{C}$

The equilibrium $\mathbf{O}_s$ is unstable (i.e., stable in reverse time), the limit cycles $\mathbf{NSC}_1$ and $\mathbf{NSC}_2$ are unstable (of the saddle type), and the 2-torus $\mathbb{T}^2$ is stable. The stability properties follow from the stability of **C** and the instability of **O**. The torus $\mathbb{T}^2$ consists of the continuum of periodic orbits since the initial phase shift between the oscillators can be chosen arbitrarily.

Now assume that the coupling strength parameter α is small and positive. Then structurally stable invariant sets (the equilibrium $\mathbf{O}_s$ and the limit cycles $\mathbf{NSC}_1$ and $\mathbf{NSC}_2$) persist and remain of the same stability type. The trajectories on the 2-torus $\mathbb{T}^2$ are structurally unstable, but this 2-torus persists under perturbation (Fenichel 1971). Typically, only a finite (and even) number of periodic orbits 'survive' on the 2-torus $\mathbb{T}^2$. Due to the symmetry of system (2), at least two invariant limit cycles exist on the 2-torus $\mathbb{T}^2$ (see the Appendix for more details): an in-phase limit cycle (**IPC**), corresponding to oscillations with zero phase shift between the identical oscillators; and an antiphase limit cycle (**APC**), corresponding to the half-period phase shift. The stability and bifurcations of these limit cycles can be investigated by numerical and asymptotic methods.

Remark 1. For $I_0 \in (-1, 0.19)$ the single oscillator has three steady states ($\mathbf{O}_1$, $\mathbf{O}_2$, $\mathbf{O}_3$) and one limit cycle **C**. Hence, for the parameter α equal to zero or a small value, the number of invariant sets of system (2) is equal to 14: $\mathbf{O}_1 \times \mathbf{O}_1, \mathbf{O}_1 \times \mathbf{O}_2, \mathbf{O}_1 \times \mathbf{O}_3, \mathbf{O}_2 \times \mathbf{O}_1, \mathbf{O}_3 \times \mathbf{O}_1, \mathbf{O}_2 \times \mathbf{O}_3, \mathbf{O}_3 \times \mathbf{O}_2, \mathbf{O}_1 \times \mathbf{C}, \mathbf{C} \times \mathbf{O}_1, \mathbf{O}_2 \times \mathbf{C}, \mathbf{C} \times \mathbf{O}_2, \mathbf{O}_3 \times \mathbf{C}, \mathbf{C} \times \mathbf{O}_3, \mathbf{C} \times \mathbf{C}$.

3.2 Bifurcation diagram for $\alpha = 0.05$

In this section we describe the evolution of the four limit cycles mentioned above when the value of the external input I_0 increases over the interval (0.2, 6.5). The equilibrium $\mathbf{O}_s$ is unstable for the same values of the parameter I_0. The bifurcation diagrams are presented in Fig. 2.

The **APC** is stable when I_0 belongs to the interval (0.2, **f**). At point **f**($I_0 = 0.42$), the **APC** becomes unstable via a pitchfork bifurcation, and a pair of stable shift-phase limit cycles ($\mathbf{SPC}_1$ and $\mathbf{SPC}_2$ with phase shifts $\pm\varphi$ between oscillators) appears on the invariant 2-torus for $I_0 >$ **f**. By analogy, the **APC** becomes stable via pitchfork bifurcation at point **h** ($I_0 = 4.39$) and gives rise to a pair of unstable limit cycles $\mathbf{SPC}_3$ and $\mathbf{SPC}_4$ on the 2-torus $\mathbb{T}^2$ for $I_0 >$ **h**. The **APC** loses stability at point **k** ($I_0 = 6.37$) via a torus bifurcation, giving rise to the torus $\mathbf{T}_a$, which exists for $I_0 >$ **k**.

The **IPC** is unstable when I_0 belongs to the interval (0.2, **g**) and becomes stable at point **g** ($I_0 = 1.66$) via a pitchfork bifurcation where the unstable **IPC** merges with the stable limit cycles $\mathbf{SPC}_1$ and $\mathbf{SPC}_2$. When I_0 increases further, the **IPC** remains stable.

The limit cycles $\mathbf{NSC}_1$ and $\mathbf{NSC}_2$ are unstable for all values of the parameter I_0 in the interval (0.2, 6.5).

Let us describe the stable dynamic regimes of system (2) for $I_0 \in (0.2, 6.5)$:

(0.2, **f**(0.42)) antiphase oscillations (**APC**), (Fig. 3a)
(**f**(0.42), **g**(1.66) two types of oscillations with the period T and the phase difference $\pm\varphi$ ($\mathbf{SPC}_1$ and $\mathbf{SPC}_2$) as I_0 increases, the phase difference φ decreases from $T/2$ to zero (Fig. 3b)
(**g**(1.66), **h**(4.39)) in-phase oscillations (**IPC**, Fig. 3c)
(**h**(4.39), **k**(6.37)) two types of oscillations: in-phase (**IPC**) and antiphase (**APC**)
(**k**(6.37), 6.5)) two types of oscillations: in-phase (IPC) and quasiperiodic ($\mathbf{T}_a$) (Fig. 3d)

The dynamics of the system above and before the interval (0.2, 6.5) can be described as follows. In the regions

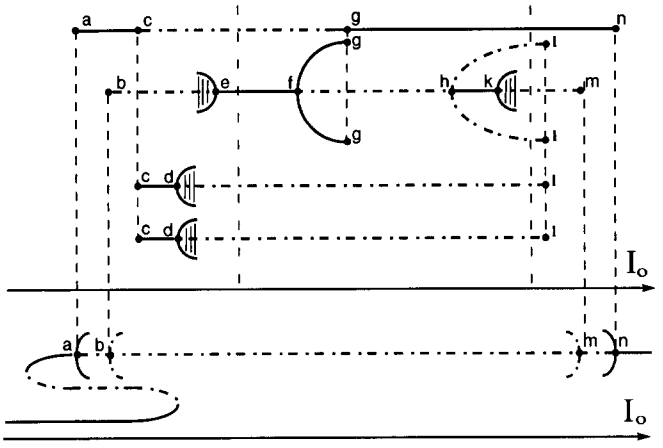

Fig. 2. Bifurcation diagrams of limit cycles (*top*) and stationary states (*bottom*) for a fixed coupling strength ($\alpha = 0.05$) and increasing I_0. A *solid line* corresponds to a stable regime, a *dash-dot line* to an unstable one. *a* ($I_0 = -0.57$), birth of an in-phase limit cycle (IPC; Andronov-Hopf bifurcation); *b* ($I_0 = -0.42$), birth of an antiphase limit cycle (APC, Andronov-Hopf bifurcation); *c* ($I_0 = -0.37$), birth of a pair of nonsymmetric limit cycles (NSC_1 and NSC_2, pitchfork bifurcation); *d* ($I_0 = -0.36$), birth of a pair of tori (T_1 and T_2, torus bifurcation); *e* ($I_0 = -0.20$), disappearance of the torus T_a (torus bifurcation); *f* ($I_0 = 0.42$), birth of a pair of shift-phase limit cycles (SPC_1 and SPC_2, pitchfork bifurcation); *g* ($I_0 = 1.66$), disappearance of the pair of shift-phase limit cycles SPC_1 and SPC_2 (pitchfork bifurcation); *h* ($I_0 = 4.39$), birth of a pair of shift-phase limit cycles (SPC_3 and SPC_4, pitchfork bifurcation); *k* ($I_0 = 6.37$), birth of a torus T_a (torus bifurcation); *l* ($I_0 = 7.01$), mergence and disappearance of a pair of shift-phase limit cycles (SPC_3 and SPC_4) and a pair of nonsymmetric limit cycles (NSC_1 and NSC_2, fold bifurcation); *m* ($I_0 = 7.09$), disappearance of an antiphase limit cycle (APC, Andronov-Hopf bifurcation); *n* ($I_0 = 7.90$), disappearance of an in-phase limit cycle (IPC, Andronov-Hopf bifurcation)

$I_0 \in (-0.57, 0.2)$ and $I_0 \in (6.5, 7.9)$, which are separated by the dash lines in Fig. 2, the system exhibits a rather complex behavior due to the coexistence of many stable regimes which undergo a number of bifurcations for small variations of I_0. For example, for $I_0 = -0.25$ one can observe two stable tori, a stable equilibrium, and two stable nonsymmetric limit cycles. Note that for $I_0 \in (-0.36, -0.20)$ the system demonstrates quasi-periodic oscillations corresponding to a trajectory on the torus.

To explain this complex behavior, let us consider the neighborhoods of the points $(-0.57, 0)$ and of the point $(7.9, 0)$ on the two-dimensional parametric plane (I_0, α). As has been mentioned above, system (1) has Andronov-Hopf bifurcations at points $I_0 = -0.57$ and $I_0 = 7.9$. Therefore, system (2) should be considered in the neighborhood of bifurcation points $(-0.57, 0)$ and $(7.9, 0)$ on the two-dimensional parametric plane (I_0, α) for small values of α. Each of these bifurcations means that two equal pairs of complex-value eigenvalues of the equilibrium $\mathbf{O}_s$ cross the imaginary axis. We do not consider the complete bifurcation diagram and the detailed picture of various phase portraits but only some bifurcations of four limit cycles for $\alpha = 0.05$ (for more details, see Aronson et al. 1990).

The stable **IPC** appears at point **a** ($I_0 = -0.57$) via Andronov-Hopf bifurcation. At point **c** ($I_0 = -0.37$), it

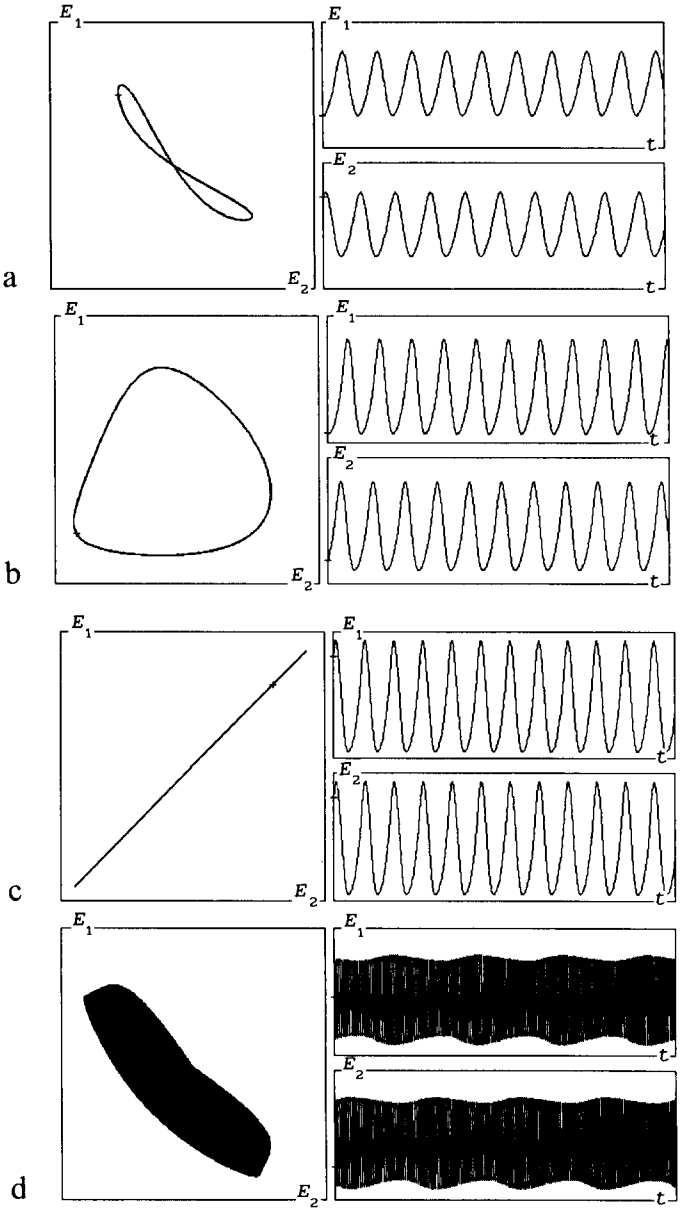

Fig. 3a–d Examples of various limit cycles and tori. **a** Antiphase limit cycle, $I_0 = 0$; **b** shift-phase limit cycle, $I_0 = 1$; **c** in-phase limit cycle, $I_0 = 2$; **d** quasiperiodic oscillations, torus T_a, $I_0 = 6.4$

loses stability due to a subcritical pitchfork bifurcation which gives rise to two stable limit cycles (**NSC_1** and **NSC_2**) for $I_0 >$ **c**. When $I_0 > 6.5$, the **IPC** is stable. It disappears via Andronov-Hopf bifurcation at point **n** ($I_0 = 7.9$).

The unstable **APC** appears at point **b** ($I_0 = -0.42$) via Andronov-Hopf bifurcation. It becomes stable at point **e** ($I_0 = -0.2$) due to a torus bifurcation (i.e., two complex multipliers cross the unit circle), and a stable torus $\mathbf{T_a}$ appears for $I_0 <$ **e**. The **APC** disappears at point **m** ($I_0 = 7.09$) via Andronov-Hopf bifurcation.

The **NSC_1** and **NSC_2** are stable for $I_0 >$ **c** ($I_0 = -0.37$) and lose stability via a torus bifurcation at point **d** ($I_0 = -0.36$), at which a pair of stable tori $\mathbf{T_1}$ and $\mathbf{T_2}$ branch out for $I_0 >$ **d**. In a small neighborhood of

$I_0 = -0.2$, the tori merge together with the stable torus $\mathbf{T_a}$, probably in the same way as that described by Khibnik et al. (1992). At point I ($I_0 = 7.01$), the pair of cycles $\mathbf{NSC_1}$ and $\mathbf{NSC_2}$ merges together with the pair of cycles $\mathbf{PSC_3}$ and $\mathbf{PSC_4}$, and these four cycles disappear.

Remark 2. The regime of antiphase oscillations described above (and other stable regimes) is robust in the following sense. Let us choose the external polarizing current I_0^1 for the first oscillator and I_0^2 for the second oscillator that corresponds to the mode of antiphase oscillations (for example, $I_0^1 \approx I_0^2 \approx 0.1$). Suppose that $\Delta I_0 = I_0^1 - I_0^2$. Then in accordance with the results of simulations, the limit cycle will also be stable for any value of ΔI_0 from the interval ($-0.1 < \Delta I_0 < 0.1$).

3.3 Bifurcations of limit cycles on the invariant torus for a weak coupling

The general tool in studies of a dynamic system with a small parameter involves asymptotic methods of expansion in series over the small parameter. The main ideas of this approach and numerical algorithm are described in the Appendix. Here we use the algorithm to study bifurcations of the limit cycles of system (2) which lie on the invariant 2-torus $\mathbb{T}^2$ as parameter α tends to zero.

Suppose a single oscillator has a stable limit cycle with the period T_0. Then by changing $t \to 2\pi t/T_0$, we obtain a 2π-periodic limit cycle. For $\alpha = 0$, system (2) has the invariant 2-torus $\mathbb{T}^2$ which is a product of the limit cycles of the oscillators. Let φ be a phase shift chosen arbitrarily at an initial moment ($0 \leqslant \varphi \leqslant 2\pi$). If the coupling strength α of system (2) is small, the invariant 2-torus $\mathbb{T}^2$ persists (Fenichel 1971), but the family of limit cycles breaks down, and only a finite number of them survives on the torus. To find which cycles will survive, one should solve the equation:

$$H(\varphi) = 0$$

where

$$H(\varphi) = \int_0^{2\pi} \langle g(u(s), u(s+\varphi)) - g(u(s), u(s-\varphi)), V^*(s) \rangle \, ds$$

Here $\langle \cdot\,, \cdot \rangle$ is the scalar product, and $V^*(s)$ is a 2π-periodical vector function.

This equation is derived in the Appendix. A solution φ of this equation corresponds to a limit cycle of system (2), existing on the invariant 2-torus $\mathbb{T}^2$ for small $\alpha > 0$. Note that $\varphi_I = 0$ corresponds to **IPC**, and $\varphi_A = \pi$ corresponds to **APC**. The other solutions (φ and $\pi - \varphi$) correspond to a pair of $\mathbf{SPC_1}$ and $\mathbf{SPC_2}$.

Figure 4a shows the bifurcation diagram of limit cycles when α tends to zero.

At point $I_0 = -0.11$, the **APC** loses stability via the pitchfork bifurcation and gives rise to a pair of stable limit cycles ($\mathbf{SPC_1}$ and $\mathbf{SPC_2}$). When I_0 increases, these cycles evolve in such way that the phase difference φ decreases gradually from π to 0.

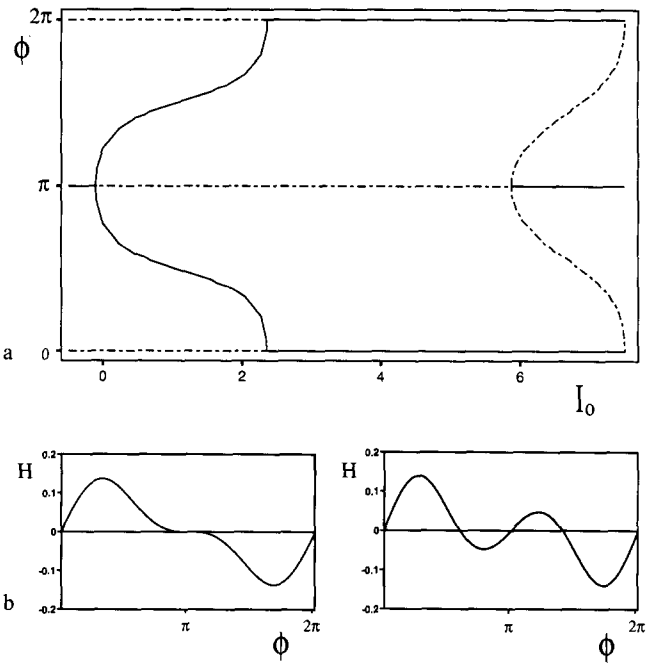

Fig. 4. a A bifurcation diagram of limit cycles as α tends to zero, constructed after solving the branching equation for various values of the parameter I_0. A *solid line* corresponds to a stable regime, a *dash-dot line* to an unstable one. **b** Function $H(\varphi)$ for various values of the parameter I_0 (*left*: $I_0 = -0.11$, *right*: $I_0 = 0.5$). The values of the φ^* at which $H(\varphi^*) = 0$ are the phase differences in the activity of two oscillators. The value $I_0 = -0.11$ corresponds to the pitchfork bifurcation of the antiphase limit cycle

Table 1. Values of the bifurcation parameter I_0

$\alpha \to 0$	$\alpha = 0.05$	Difference
−0.11	**f** (0.42)	−0.53
2.37	**g** (1.66)	0.71
5.87	**h** (4.39)	1.48

At point $I_0 = 2.37$, two branches of the limit cycles $\mathbf{SPC_1}$ and $\mathbf{SPC_2}$ merge with the unstable **IPC** (pitchfork bifurcation), and for $I_0 > 2.37$, the **IPC** becomes stable.

The pitchfork bifurcation occurs at $I_0 = 5.87$. Here the unstable **APC** gives rise to a pair of unstable limit cycles ($\mathbf{SPC_3}$ and $\mathbf{SPC_4}$), and the **APC** becomes stable for $I_0 > 5.87$.

Remark 3. The bifurcation diagram is based on calculating the function $H(\varphi)$ and represents only limit cycles on the invariant torus. For the same I_0, the system can have other cycles outside the torus.

Remark 4. The pitchfork bifurcations of the **IPC** and **APC** when α tends to zero are similar to the bifurcations described in Sect. 3.2. The only difference involves the values of the bifurcation parameter I_0 (Table 1).
To explain the rather large difference, let us consider a two-dimensional parametric plane (I_0, α). It can be

shown that near $\alpha = 0$, the pitchfork bifurcation value $I_0(\alpha)$ satisfies the following asymptotic expression:

$$I_0(\alpha) = I_0(0) + K\alpha^{1/2}$$

where K is a constant. It follows from this formula that in the neighborhood of $\alpha = 0$, the bifurcation value of the parameter I_0 changes drastically with a small variation of α. Thus, the bifurcation value of the parameter I_0 is rather sensitive to small variations of the coupling strength α.

4 Discussion

The dynamic behavior of a system of two electrically coupled oscillatory neurons exhibits a variety of stable oscillatory regimes, each characterized by the phase shift between oscillator activities. The phase shift may range from zero to half the period, depending on the value of the polarizing current. By varying the value of the external polarizing current at each of the oscillators, one can observe smooth transitions between antiphase and in-phase oscillations.

The model represents a simple example of a neural network with multiple oscillatory modes. The transition from one regime to another is performed by varying the polarizing current under a fixed small value of the electrical coupling. This example is closely related to the study of the mechanisms underlying CPGs (Grillner and Matsushima 1991). In studies of CPG mechanisms, the problem of control over the transitions between various patterns is of great interest.

The variation of the external polarizing current in our model could reflect changes in the membrane conductivity induced, for example, by neurotransmitters. The role of modulatory influences on the output patterns is one of the key problems in CPG investigations (Marder et al. 1987; Harris-Warrick 1988; Cazalets et al. 1990).

A hypothesis by Marder et al. (1987) suggests that one and the same neural network may generate different patterns, depending on the modulatory substances present. Thus, the transitions from one pattern to another in the pyloric rhythm generator of the stomatogastric ganglion of lobsters take place because the modulators act differently on different neurons of the system (Eisen and Marder 1984; Marder and Eisen 1984; Marder et al. 1987), in effect restructuring the network.

The results presented here show that transitions between regimes can occur in a network without differentially changing the intrinsic activities or varying the strengths of coupling within the network. In our model, the connections and their strengths are kept constant. The polarizing current is changed in exactly the same way for both cells. Thus, there is no restructuring of the network. Nevertheless, continuous changes of modulator concentrations in the surrounding solution can lead to the transition from the antiphase oscillatory regime to the in-phase one.

In addition, there is a concentration at which the antiphase and in-phase regimes coexist, and the choice between these regimes is determined by the initial conditions. In summary, even the simplest network of two electrically coupled, endogenous oscillators can exhibit a dynamic behavior which is of interest with respect to the study of more complex neuronal networks.

Appendix

A.1 Malkin's theorem on branching limit cycles in a system of two weakly coupled oscillators

Let us present a simple general framework for finding limit cycles and determining their stability when the coupling parameter α is small enough $0 \leqslant |\alpha| \ll 1$. Assume that the dynamics of the system is described by

$$\begin{aligned} dx_1/dt &= f(x_1) + \alpha g(x_1, x_2) \\ dx_2/dt &= f(x_2) + \alpha g(x_2, x_1) \end{aligned} \tag{3}$$

Here $x_k \in \mathbb{R}^n$ are phase variables of the kth oscillator ($k = 1, 2$); $f(x)$ is a smooth vector-function describing the dynamics of a single oscillator:

$$dx/dt = f(x) \tag{4}$$

where $x \in \mathbb{R}^n$; $g(x_1, x_2)$ is a smooth vector-function determining the structure of oscillator coupling.

Suppose that $x_0(t)$ is a stable periodical solution to (4) with the (minimal) period T_0. Then for $\alpha = 0$, it corresponds to the following one-parameter family of periodical solutions to system (3):

$$Z_\varphi(t) = (x_0(t), x_0(t + \varphi)) \tag{5}$$

where the parameter φ characterizes a phase difference in the oscillations of the uncoupled oscillators, $0 \leqslant \varphi \leqslant T_0$.

Family (5) of the closed orbits Z_φ covers continuously the invariant 2-torus $\mathbb{T}^2 = x_0 \times x_0$, which is the direct product of two identical limit cycles of the single oscillators. For sufficiently small values of $\alpha \neq 0$, the 2-torus $\mathbb{T}^2$ persists (Fenichel 1971), but family (5) breaks down so that only a finite number of limit cycles survives on $\mathbb{T}^2$. More precisely, the following theorem is valid (Malkin 1956; Blehman 1981).

Malkin's theorem. Let system (4) have a stable limit cycle Z^*_φ and the conditions

$$H(\varphi^*) = 0, \quad H'(\varphi^*) \neq 0 \tag{6}$$

hold for some value $\varphi = \varphi^*$, where

$$H(\varphi) = \int_0^{T_0} \langle g(x_0(s), x_0(s - \varphi)) - g(x_0(s), x_0(s + \varphi)), v^*(s) \rangle ds \tag{7}$$

here $\langle \cdot , \cdot \rangle$ is the standard scalar product in $\mathbb{R}^n$; $v(t) = dx_0(t)/dt$ and the function $v^*(s)$ is determined below. Then:

1. System (3) has a unique limit cycle Z_α in the small neighborhood of Z^*_φ when α is sufficiently small.

2. The stability of Z_α is defined by the sign of $\mu = H'(\varphi^*)$: if μ is negative, then Z_α is stable; if μ is positive, then Z_α is unstable.

In (7), the function $v^*(t)$ is a solution to the boundary value problem:

$$dv^*/dt = -A(t)^T v^* \tag{8a}$$

$$v^*(0) = v^*(T_0) \tag{8b}$$

where $A(t) = \partial f(x_0(t))/\partial x$; the normalizing condition for the vector-function $v^*(t)$ is written as:

$$\int_0^{T_0} \langle v(s), v^*(s)\rangle ds = 1 \tag{9}$$

All solutions to (6) lie symmetrically on a circle $\mathbb{S}^1$ (mod T_0) and are always arranged in pairs: $\varphi_1^* + \varphi_2^* = T_0$. Note that (6) always has the trivial solutions $\varphi^* = 0$ and $\varphi^* = T_0/2$, corresponding to the in-phase oscillations

$$x_k^I(t;\alpha) \equiv x_k^I(t + T(\alpha);\alpha),\ x_1^I(t;\alpha) \equiv x_2^I(t;\alpha), \quad k = 1, 2$$

and antiphase oscillations

$$x_k^A(t;\alpha) \equiv x_k^A(t + T(\alpha);\alpha),\ x_1^A(t;\alpha)$$
$$\equiv x_2^A(t + T(\alpha)/2;\alpha), \quad k = 1, 2$$

where $T(\alpha) = T_0 + O(\alpha)$ is the period of oscillations for $\alpha > 0$.

The nontrivial pair of solutions $\varphi_1^* + \varphi_2^* = T_0$ corresponds to a pair of phase shift oscillations

$$x_k^{s1}(t;\alpha) \equiv x_k^{s1}(t + T(\alpha);\alpha),\ x_1^{s1}(t;\alpha)$$
$$\equiv x_2^{s1}(t + \varphi_1^*;\alpha), \quad k = 1, 2$$
$$x_k^{s2}(t;\alpha) \equiv x_k^{s2}(t + T(\alpha);\alpha),\ x_1^{s2}(t;\alpha)$$
$$\equiv x_2^{s2}(t + \varphi_2^*;\alpha), \quad k = 1, 2$$

where $T(\alpha) = T_0 + O(\alpha)$ is the period of oscillations for $\alpha > 0$.

A.2 A sketch of the numerical algorithm for the function H computation

Once a stable periodic solution $x_0(t)$ to (4) is found, the calculation of $H(\varphi)$ can be made in the following manner:

1. The periodic vector-function $v(t) = f(x_0(t))$ is calculated immediately.
2. To obtain the periodic vector-function $v^*(t)$ fulfilling (9), one should solve the boundary value problem (8).
3. The integral (7) can be computed using Simpson's method.

The only item of this algorithm which can present some numerical difficulties is the second one.

Given the nondegenerate periodic solution $x_0(t)$, there is a unique solution to (8) up to an arbitrary constant (all the simplest theoretical results needed in this Appendix can be found in Hartmann 1964).

To solve problem (8), one should obtain the fundamental matrix M of (8a). To make this, one needs to solve (8a) with the following set of initial values:

$$\hat{v}_k(0) = (0, \ldots, 1, \ldots, 0)^T, \quad (k = 1, \ldots, n)$$

where the unit occupies the kth initial value vector position, and the other positions of that vector are occupied by zeros.

Fundamental matrix M is constructed of the vector columns: $M = [\hat{v}_1(T_0), \ldots, \hat{v}_n(T_0)]$, where $\hat{v}_k(T_0)$ is the kth solution to (8a) at $t = T_0$.

Using a standard linear algebra package (e.g., LINPACK by Dongarra et al. 1978), one can find the eigenvector $\mathbf{u}$ of M: $M\mathbf{u} = \mathbf{u}$. Then the solution $\hat{v}^*(t)$ to (8a) such that $\hat{v}^*(0) = \mathbf{u}$ satisfies (8b) and $\hat{v}^*(t) = \hat{v}^*(t)/c$, where $c = \int_0^{T_0} \langle v(s), v^*(s)\rangle ds$, fulfills (9).

Acknowledgements. We are grateful to Prof. E. E. Shnol for helpful discussions and Dr. J. Dean for reading the manuscript. G.S.C. and E.V.N. were supported by the G. Soros International Science Foundation. R.M.B. was supported by the James S. McDonnell Foundation (grant no. 93-9).

References

Aronson DG, Ermentrout GB, Kopell N (1990) Amplitude response of coupled oscillators. Physica D 41:403–449

Arshavsky YuI, Belozerova IN, Orlovsky GN, Panchin YuV, Pavlova GA (1985) Control of locomotion in marine mollusk *Clione limacina*. III. On the origin of locomotory rhythm. Exp Brain Res 58:263–272

Blehman II (1981) Sychronization in nature and engineering (in Russian). Nauka, Moscow

Borisyuk GN, Borisyuk RM, Khibnik AI (1992) Analysis of oscillatory regimes of a coupled neural oscillator system with application to visual cortex modeling. In: Taylor JG, Caianiello RM, Cotterill RMJ (eds) Neural network dynamics. Springer, Berlin Heidelberg New York, pp 208–225

Cazalets JR, Nagy F, Moulins M (1990) Suppressive control of the crustacean pyloric network by a pair of identified interneurons. I. Modulation of the motor pattern. J Neurosci 10:448–457

Collins JJ, Stewart IN (1993) Coupled nonlinear oscillators and the symmetries of animal gaits. J Nonlin Sci 3:349–392

Constantine-Paton M, Cline HT, Debski E (1990) Patterned activity, synaptic convergence, and the NMDA receptor in developing visual pathways. Annu Rev Neurosci 13:129–154

Cruse H (1990) What mechanisms coordinate leg movement in walking arthropods? Trends Neurosci 13:15–21

Dermietzel R, Spray D (1993) Gap junction in the brain: where, what type, how many and why? TINS 16:186–192

Dongarra JJ, Bunch JR, Moler CB, Stewart GW (1978) LINPACK users guide. SIAM Publications, Philadelphia

Eisen JS, Marder E (1984) A mechanism for production of phase shifts in a pattern generator. J Neurophysiol 51:1375–1393

Ermentrout GB, Kopell N (1991) Multiple pulse interactions and averaging in systems of coupled neural oscillators. J Math Biol 29:195–217

Fenichel N (1971) Persistence and smoothness of invariant manifolds for flows. Indiana Univ Mathematics J 21:3

Getting PA (1988) Comparative analysis of invertebrate central pattern generators. In: Cohen AH, Rossignol S, Grillner S (eds) Neural control of rhythmic movements in vertebrates. Wiley, New York, pp101–127

Grillner S, Matsushima T (1991) The neural network underlying locomotion in lamprey – synaptic and cellular mechanisms. Neuron 7:1–15

Harris-Warrick RM (1988) Chemical modulation of central pattern generators. In: Cohen AH, Rossignol S, Grillner S (eds) Neural control of rhythmic movements in vertebrates. Wiley, New York, pp286–331

Hartmann F (1964) Ordinary differential equations. Wiley, New York

Hindmarsh JL, Rose RM (1982) A model of the nerve impulse using two first-order differential equations. Nature 296:162–164

Hindmarsh JL, Rose RM (1984) A model of neuronal bursting using three coupled first order differential equations. Proc R Soc Lond B 221:87–102

Kawato M, Sokabe M, Suzuki R (1979) Synergism and antagonism of neurons caused by an electrical synapse. Biol Cybern 34:81–89

Khibnik AI, Borisyuk RM, Roose D (1992) Numerical bifurcation analysis of a model of coupled neural oscillators. Int Ser Num Math 104:215–228

Khibnik AI, Kuznetsov YuA, Levitin VV, Nikolaev EV (1993) Continuation techniques and interactive software for bifurcation analysis of ODEs and iterated maps. In: Proceedings of Advanced NATO Workshop on Homoclinic Chaos. Physica D V.62 (1–4):360–367

Kopell N (1988) Toward a theory of modelling central pattern generators. In: Cohen AH, Rossignol S, Grillner S (eds) Neural control of rhythmic movements in vertebrates. Wiley, New York, pp369–413

Malkin IG (1956) Some problems of the theory of nonlinear oscillations (in Russian). Gostehizdat, Moscow

Marder E, Eisen JS (1984) Electrically coupled pacemaker neurons respond differently to same physiological inputs and neurotransmitters. J Neurophysiol 51:1362–1374

Marder E. Hooper SL, Eisen JS (1987) Multiple neurotransmitters provide a mechanism for the production of multiple outputs from a single neuronal circuit. In: Edelman GM, Gall WE, Cowan MW (eds) Synaptic function, NRF. Wiley, New York, pp305–327

Marder E, Abbot LF, Kepler T, Hooper SL (1992) Modification of oscillator function by electrical coupling to nonoscillatory neurons. In: Basar E, Bullock TH (eds) Induced rhythms in the brain. Birkhauser, Boston, pp287–296

Müller U, Cruse H (1991) The contralateral coordination of walking legs in the crayfish *Astacus leptodactylus*. II. Model calculations. Biol Cybern 64:437–446

Rand RH, Cohen AH, Holmes PJ (1988) Systems of coupled oscillators as models of central pattern generators. In: Cohen AH, Rossignol S, Grillner S (eds) Neural control of rhythmic movements in vertebrates. Wiley, New York, pp333–367

Schöner G, Jiang WY, Kelso JAS (1990) A synergetic theory of quadrupedal gaits and gait transitions. J Theor Biol 142:359–391

Selverston AI, Moulins M (1985) Oscillatory neural networks. Annu Rev Physiol 47:29–48

Taga G, Yamaguchi Y, Shimizu H (1991) Self-organized control of bipedal locomotion by neural oscillators in unpredictable environment. Biol Cybern 65:147–159

Yang XD, Korn H, Faber DS (1990) Long-term potentiation of electrotonic coupling at mixed synapses. Nature 348:542–545

Yuste R, Peinado A, Katz LC (1992) Neuronal domains in developing neocortex. Science 257:665–668